RECENT DEVELOPMENTS OF EDDY CURRENT INSPECTION SIMULATOR

N. Nakagawa, M. Garton, J. C. Moulder, J. H. Rose, and J. Xu
Center for NDE
Iowa State University
Ames, IA 50011

INTRODUCTION

This paper reports on development of simulation software for eddy current (EC) inspections.

The purpose of such software development is threefold: First, the simulator serves as an analysis tool for NDE researchers to understand underlying physical processes on computers. Second, it provides a vehicle for software technology transfer to practicing NDE engineers and to component designers. Third, it can become an integral part in (or the NDE module of) the unified life-cycle environment, serving as the NDE technology resource.

The simulator development starts with existing sets of underlying physics models and their software implementations. Our approach is to take them, and to incorporate them into the simulator which provides stream-lined, user-friendly environments, where a user, who may or may not be an NDE expert, can run the physics model codes and get benefit of the analysis capabilities.

The simulator reported here has been under development for these purposes. In addition to the EC simulator presented here, software simulators may be found in other NDE modalities [1,2].

In the next section, we describe briefly a list of physics models made available to the simulator developments. The subsequent sections show two versions of EC simulator implementations. The last section is for conclusions.

PHYSICS MODELS

In this section, we will list physics models which have been, or are planned to be, incorporated into the EC simulator.

Half Space and Metal Multi-Layers

The first class of the model applies to metal half space and multi-layers, scanned over with a solenoid coil (Fig. 1). This class of the eddy current system is unique in the sense

Review of Progress in Quantitative Nondestructive Evaluation, Vol 16
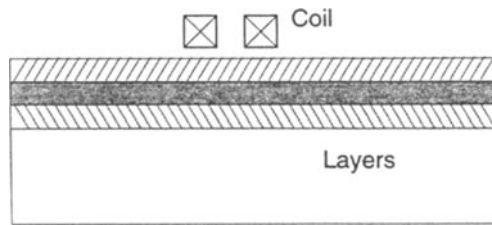Edited by D.O. Thompson and D E Chimenti, Plenum Press, New York, 1997

959

Figure 1. Illustration of a metal multi-layer object and a solenoid coil. Each layer of finite thickness can have separate material properties. Some layers may be set to be air when considering corrosion detection.

that it admits analytical, closed-form solutions [3,4]. It is an ideal example, therefore, for illustrating the basic nature of eddy current phenomena to non-experts. Furthermore, the model has been proven useful in practical applications of layer-sizing and corrosion detection algorithms via the swept-frequency method [5,6]. It was this model that was first incorporated into the simulator. The code runs with near real-time response thanks to the analytical solution. The physics model itself has been further extended so that it applies to time-domain phenomena. In view of the success of the pulsed eddy current instrument, the time-domain code will become important, and thus is a prime candidate for future inclusion into the simulator.

Crack in Half Space and Plate Geometry

The second class of the models to mention here is the crack detection model. A prototypical case is a surface-breaking tight crack on the half space specimen, with a solenoid coil scanning over the crack region (Fig. 2). This is the most fundamental crack detection geometry, and of both conceptual and practical importance as a benchmark example. The code to compute the crack impedance signals for this system has been available for years [7]. The code has been extended later so that it can also compute the electric field (i.e. eddy current) everywhere including the vicinity of the crack. This version of the crack code has been used in the simulator to date. The physics model has been further updated and revised since then. The most recent version allows the specimen to be a finite-thickness plate, and a crack to occur on either side of the plate surface with respect to the coil side. Besides, the crack can be a collection of smaller cracks, roughly aligned in line with possible offsets. These are particularly useful features when investigating steam-generator tubing inspections. The updated physics code may be included into the simulator in the future.
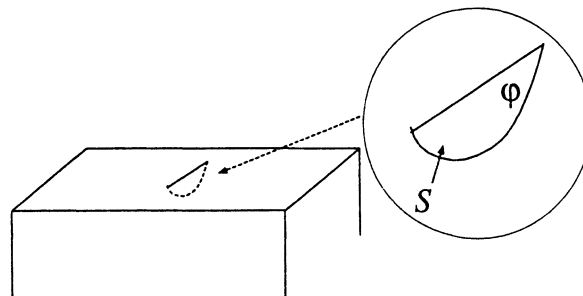

Figure 2. A crack on the surface of a block specimen.

General 3D EC BEM Code

The third category of the models is the most advanced in dealing with general system geometry, and currently under development [8]. The code is designed to be as robust as applicable to industrial EC inspections. This code is yet to be incorporated into the simulator for various reasons: the code is relatively new, and the computational procedure is inevitably involved. Also, the code requires intensive computation to yield results. Nevertheless, the simulator development plan includes the implementation of the 3D BEM code in the future, because there is an obvious benefit if the BEM code is attached to the user-friendly simulator environment which can guide the user through the complex computational procedure.

EC Instrument Simulation

Fourth, we describe the EC instrument simulation. This concerns empirical modeling, and, strictly speaking, is not a physical model. It is nevertheless included here for convenience. Physics models such as those above predict probe impedance in the absolute sense (in ohms), while most EC measurements are done by analog instruments that yield relative readings in volts. Lepine and Moulder developed an instrument calibration procedure by which the transfer function from voltage to impedance can be determined empirically [9]. In the simulator, we use the transfer function in the reverse order, translating the physics model output (in ohms) to the voltage readout as ordinary instruments provide. The transfer functions determined for the selected instruments in Ref. 9 were actually incorporated into the simulator for instrument simulation.

EC SIMULATOR, FIRST VERSION

The first version of the EC simulator was developed by J. Xu, and written for the X-Windows platform. The graphical user interface (GUI) code implements the metal multi-layer code and the half-space crack code as physics engines. (See the previous section.) This is hence useful particularly for studying layer-sizing and corrosion inspection applications. We focus our discussion here to the multi-layer mode, since the later version of the simulator is available for the crack modeling. (See the subsequent section).

After a few steps from startup, the simulator user encounters the main setup window similar to the one in Fig. 3. Here, the user can specify the parameters such as coil parameters, material parameters, and other specimen parameters. The picture happens to show the corrosion detection mode, and hence the amount of corrosion is another parameter to set. In the general layer mode, the user can set the layer parameters such as the numbers of layers, material and thickness of each layer, *etc.*

The output is coil impedances, and the user has options to compute them as functions of frequencies, corrosion amounts, lift-off, *etc.* By default, the output is plotted in the main plotting window (Fig. 4), or, optionally, can be sent to a file.

Figure 4 actually contains important physical results, the key feature to the swept-frequency corrosion detection approach [5,6]. Notice the characteristic zero-crossing of the real parts in Fig. 4. It was pointed out [5,6] that the zero frequency gives an accurate measure for layer sizes and/or corrosion amounts. Those interested in the physics are encouraged to read the papers. Here, it should be emphasized that the primary usage of the simulator is exhibited: The modeling helps NDE researchers to understand the fundamentals of the NDE process. The simulator, in turn, makes the same numerical results used by the researcher available to any non-experts readily.
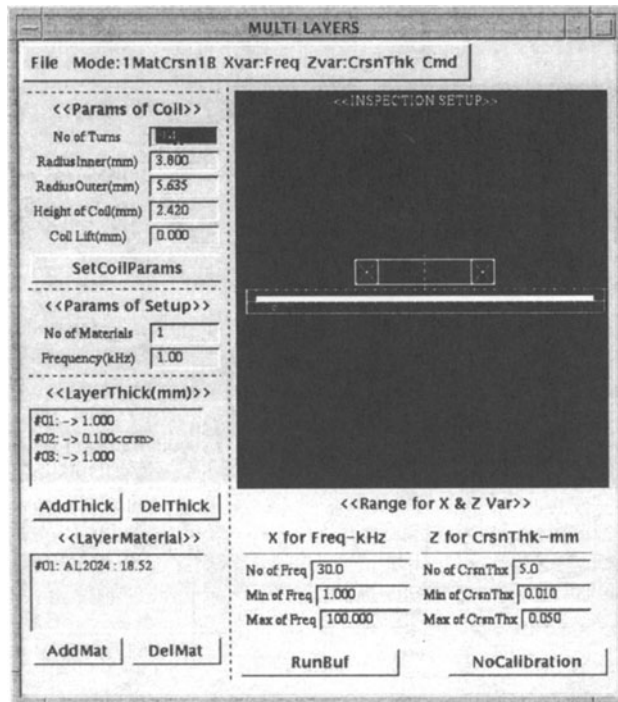
Figure 3. Screen capture of the simulator main setup window. This particular window is in the corrosion mode. In this case, the user can set various parameters such as coil parameters, plate material properties, plate thickness, the amount of corrosions, and the frequency range if applicable.
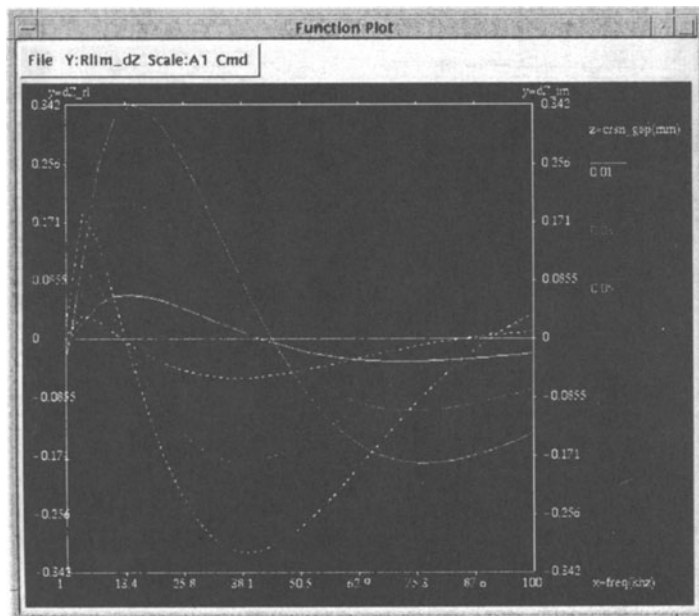

Figure 4. A typical example of the main plotting window. This particular one shows coil impedance (real parts) plotted against a range of frequencies for several corrosion amounts. Observe the characteristic zero crossings of the curves.

As discussed in Introduction, the simulator is not only a researcher's tool, but also can be reconfigured to be useful for NDE practitioners. Let us, for example, consider the conventional corrosion detection procedure via the EC instruments, and try to simulate it. The standard procedure do not involve either swept frequencies, or absolute impedance measurements. Instead, they use single frequency measurements with analog instruments. Hence, it is necessary to prepare calibration specimens so that relative measurements against the calibration data can be performed. We have actually implemented a mockup procedure into the simulator. Figure 5 illustrates the type of a virtual calibration specimen the simulator user can construct. Specifically, Figure 5A shows that the calibration specimen may consist of a pair of plates, one of which may have known amounts of thinnings. In the calibration setup window, the simulator user can specify parameters such as material properties, the number of corroded areas, and each of the corrosion amounts, in addition to the usual parameters (Fig. 3). When run, the code computes the air-gap signals (Fig. 5B) and the calibration signals (Fig. 5C), and uses the results to rotate and scale the impedance plan, as shown in Fig. 6, so that the calibration points (or more precisely the quadrature components of them) are distributed in the full range of the plot window. The calibration steps programmed here is an approximate mockup of the actual calibration procedure inspectors are required to follow before field inspections. The simulator user then proceeds to compute signals for target corrosion inspections. In stead of plotting the results as before (Fig. 4), the code plots the result in the calibrated impedance plane, relative to the calibration points. If the target points happen to fall outside the region, then the user should go back and "re-design" the calibration parameters until all the target signals fall safely within the range spanned by the calibration points.

EC SIMULATOR, CURRENT VERSION

The current version the EC simulator has been developed by M. Garton and his team of students. The features of their code include the use of X-FORM, OpenGL, and the C++ language. The code development emphasizes the graphical capabilities such as 3D visualization and built-in scan-plan generation. The code is show to transfer well from a platform to platform where the above software tools are available.

(A)

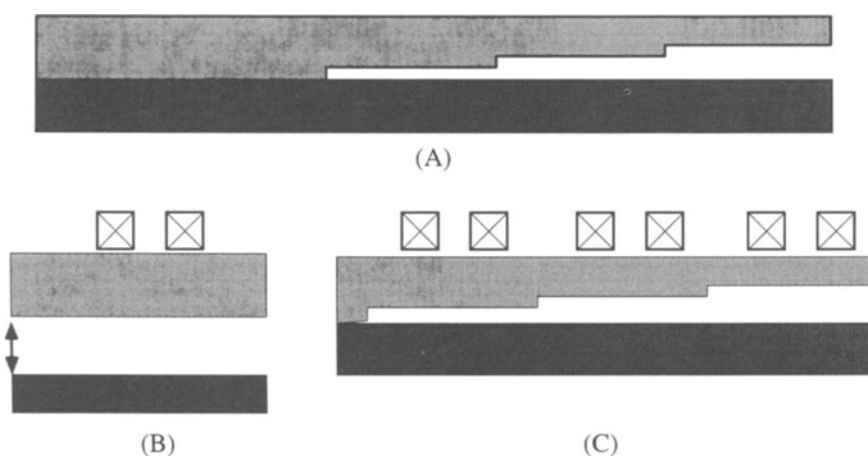(B)   (C)

Figure 5. Illustrations for conceptual calibration specimen for corrosion detection. (A) shows the pair of plates with artificial metal losses, (B) indicates the definition of the "air gap" signals, and (C) indicates the coil positions to set for each calibration calculation.
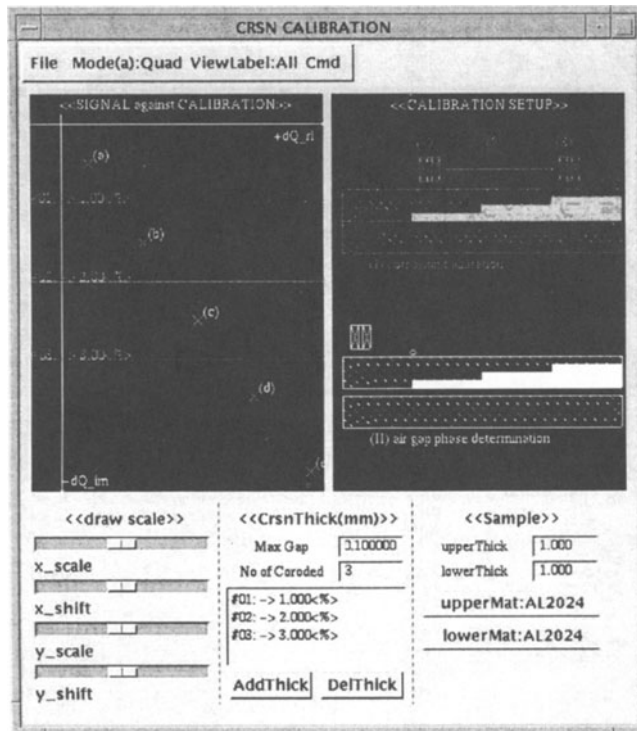
CRSN CALIBRATION

File Mode(a):Quad ViewLabel:All Cmd

<<SIGNAL against CALIBRATION>>

+dQ_rl

(a)

(b)

(c)

(d)

-dQ_im

<<CALIBRATION SETUP>>

(II) air gap phase determination

<<draw scale>>

x_scale

x_shift

y_scale

y_shift

<<CrsnThick(mm)>>

Max Gap   3.100000
No of Coroded   3

#01: -> 1.000<%>
#02: -> 2.000<%>
#03: -> 3.000<%>

AddThick   DelThick

<<Sample>>

upperThick   1.000
lowerThick   1.000

upperMat:AL2024

lowerMat:AL2024

Figure 6. Simulator implementation of the calibration concept. The right window indicates the current calibration specimen setup, which the user can modify in the setup area. When run, the code rotate and scale the plot area (left) so that the calibration points will spread in the window. The plot also contains the target corrosion signals which fall properly in-between the calibration points.

Figures 7 and 8 illustrate snap shots of user screens. The interface design follows that of UTSIM [2], consisting of the menu bar, the setup panel, and the display area. This version has implemented the instrument simulation, which may or may not appear above right, depending on the user choice. Computed impedance can be mapped on the part surface (the tubing in Fig. 7). Figure 8 illustrates field computation results, displayed via the color-coded map in the part body. When the instrument simulation is on, the impedance results are translated by the transfer function, and displayed both in the strip chart form and in the complex impedance plane (the Lissajous pattern).

Since the code is under active development, the scope of the implemented physics models is changing. In the first phase, the code has incorporated the half-space field and impedance computation of Dodd and Deeds [3], and the half-space crack code with both impedance and field computation capabilities [8]. In the next phase of the development, the code is planned to include more options and physics engines made available for integration.
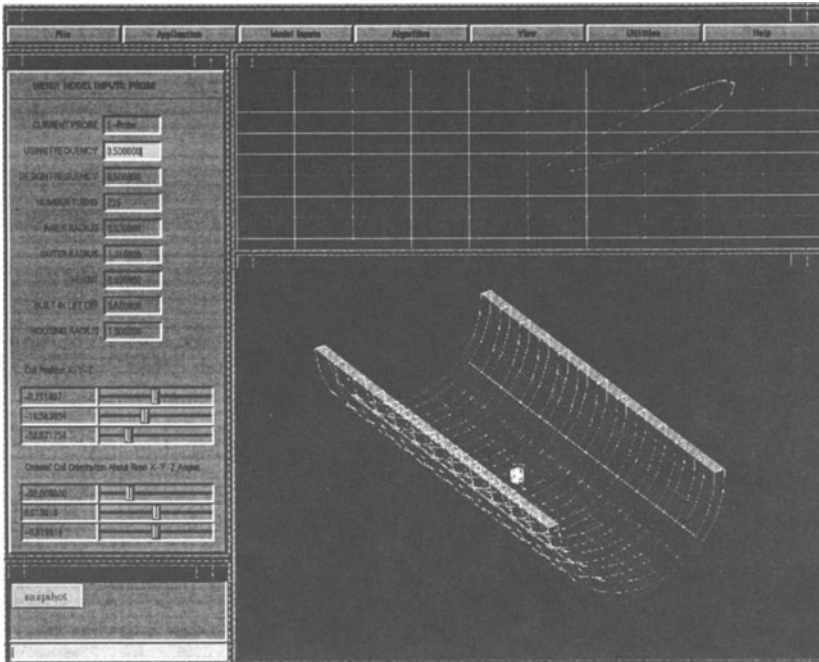
Figure 7. Captured screen of the latest EC simulator code. This picture features a typical design of the control panels, the 3D visualization window, and the EC instrument simulator window (above, right). Computed impedance can be both mapped on the part surface (tubing in this example) and displayed as a Lissajous plot and as the strip chart form.
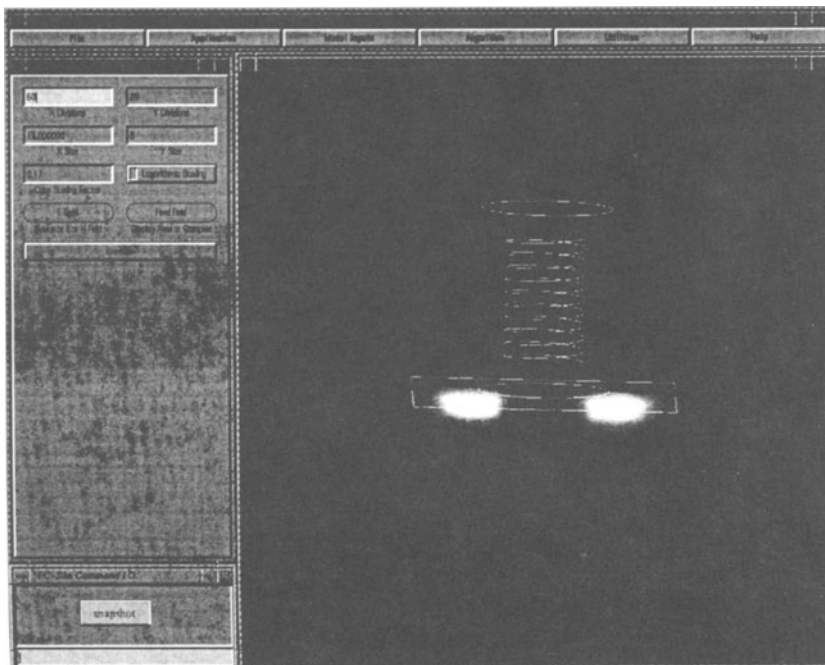

Figure 8. Color-coded display of the computed electric field (eddy current) distribution under the metal surface. The spiral line represents the size and position of the probe coil. This particular result is for a non-crack case, although similar field results can be obtained and displayed when a crack is present.

965

CONCLUSIONS

In conclusion, two versions of EC inspection simulator software are presented. They are X-Window-based simulators that provide the user with interactive, friendly interface, through which various underlying physics models can be accessed. The list of available physics models are presented in the second section above. At present, the simulators have implemented the models of basic geometry such as metal half space and multi-layered objects. Users can choose an EC inspection problem of interest among those implemented, customize input parameters, and run the code to examine the inspection performance, in terms of the predicted probe impedance mostly, and in some cases of eddy current distributions in the part body.

The simulator development presented here is planned to continue toward inclusion of more capabilities in the basic models, as well as of more advanced models of broader applicability.

ACKNOWLEDGMENTS

REFERENCES

1. J. Xu, F. Inanc, T. Aljundi, T. Jensen, and J. Gray, "Recent developments in the X-ray Radiography Simulation Code: XRSIM," in *Review of Progress in QNDE*, this volume.
2. M. Garton, T. A. Gray, and A. Minachi, "Refining Ultrasonic Inspections Using a Simulation Software Package, UTSIM," in *Review of Progress in QNDE*, this volume.
3. C. V. Dodd, and W. E. Deeds, J. Appl. Phys. 39, 2829 (1968).
4. C. C. Cheng, C. V. Dodd, and W. E. Deeds, Int. J. Nondestr. Test. 3, 109 (1971).
5. E. Uzal, J. C. Moulder, and J. Rose, J. Appl. Phys. 74, 2076 (1993).
6. S. Mitra, P .S. Urali, E. Uzal, J. H. Rose, and J. C. Moulder, in *Review of Progress in QNDE*, Vol. 12, eds. D. O. Thompson and D. E. Chimenti (Plenum, New York, 1993), p. 2003.
7. N. Nakagawa, in *Review of Progress in QNDE*, Vol. 8, eds. D. O. Thompson and D. E. Chimenti (Plenum, New York, 1989), p. 245.
8. N. Nakagawa, S. Ghanekar, D. Lehther, Y. Liu, J. C. Moulder, A. N. S. Prasad, F. Rizzo, J. C. Chao, "Progress in eddy current modeling via the boundary element method," in Review of Progress in QNDE, this volume.
B. A. Lepine and J. C. Moulder, in *Review of Progress in QNDE*, Vol. 14, eds. D. O. Thompson and D. E. Chimenti (Plenum, New York, 1995), p. 2301.